



SEISMIC FRAGILITY ANALYSIS OF C-BENT PIERS IN METRO VIADUCTS

D.C. Rai⁽¹⁾, P. Srivastava⁽²⁾

⁽¹⁾ Professor, Department of Civil Engineering, Indian Institute of Technology Kanpur, Kanpur 208016, India, dcrai@iitk.ac.in

⁽²⁾ Former Graduate Student, Department of Civil Engineering, Indian Institute of Technology Kanpur, Kanpur 208016, India, parulsri9@gmail.com

Abstract

C-bent piers have an unequal horizontal cantilever on both sides of the vertical column and the girder is placed at an eccentricity from the centre of the column. They are widely used in Indian metro viaducts at places of turning of the track or due to scarcity of space for placing piers at the median of the road. Horizontal earthquake loads significantly add to the already large flexural demands on these piers due to gravity loads. This makes them extremely vulnerable to large inelastic deformations even at low levels of shaking. In extreme cases, it may even lead to failure by toppling in the direction of eccentricity. The residual displacement undergone by the pier is an important parameter to assess its reparability after an earthquake.

In order to achieve zero permanent drift for a design level earthquake, current design proposals suggest that the ratio of difference in moment capacities (*i.e.*, for overturning in the direction of eccentricity and in the opposite direction) and the eccentric moment due to gravity loads, that is, factor β , should be taken as 2. However, such a high value of β was found to be impractical for the Indian metro specifications. Since the piers are allowed to undergo some residual displacements according to acceptable tolerance levels, a more reasonable value of $\beta = 1$ was adopted for design of C-bent piers.

To assess the non-linear behavior of C-bent piers, incremental dynamic analysis (IDA) was performed using non-linear time history analysis (NLTHA) by applying a set of 20 ground motions on the bridge configurations. The results of NLTHA were further subjected to regression analysis using which the fragility curves for C-bent piers with varying eccentricity were developed. It was seen that C-bent piers designed with $\beta = 1$ performed well for the design PGA levels up to 0.36g as per Indian Standards, with residual displacements similar to permissible construction tolerances. Also, for their reliable performance, the maximum loading eccentricity for C-bent piers should be limited to the depth of the pier in the direction of eccentricity.

Keywords: C-bent piers; Bridge; Metro viaducts; Seismic fragility



1. Introduction

C-bent piers are widely used at places of turning of the track of the train on curves or due to space constraint for placement of piers right beneath the girders. C-bent piers (also referred to as inverted-L piers) have unequal horizontal cantilevers on both sides of the vertical column. The weight of the superstructure, P , supported on a C-bent pier acts at an eccentricity, e , from its centre, resulting in large eccentric moment, $M_E (= P.e)$, at the base of the pier, as shown in Fig. 1. This causes a tendency of the pier to deform predominantly in the direction of eccentricity due to post elastic-stiffness degradation owing to $P-\Delta$ effects [1]. During earthquakes, overturning moments due to seismic loads may get added to the already large flexural demands at the base of the C-bent pier, making them extremely vulnerable to damage during earthquakes.

In order to overcome this tendency to deform in the direction of eccentricity, C-bent piers are often designed with more reinforcing steel on the face of the column opposite to the direction of eccentricity referred to as the eccentric tension side (ETS) than the face of the column in the direction of eccentricity, referred to as the eccentric compression side (ECS) [2]. The difference in strength of the pier for overturning in the direction of the eccentricity and the opposite direction is given by Eq. (1).

$$\beta = \frac{M^+ - M^-}{M_E} \tag{1}$$

where, M^+ is the moment capacity in the direction of eccentricity causing tension on ETS and M^- is the moment capacity in the opposite direction causing compression on ETS (Fig. 2). The factor β can be interpreted graphically as shown in Fig. 3.

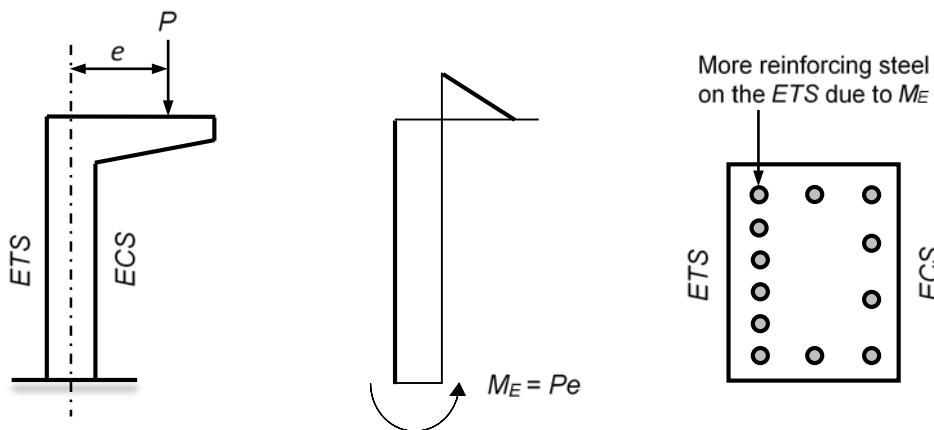


Fig. 1 – Eccentric moment, M_E and the design reinforcement of the cross-section

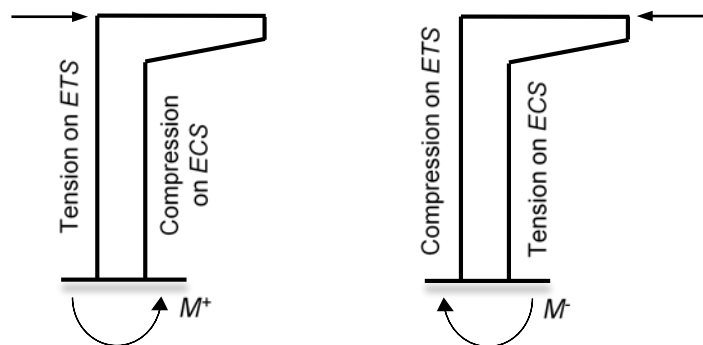


Fig. 2 – Nomenclature of moment capacities

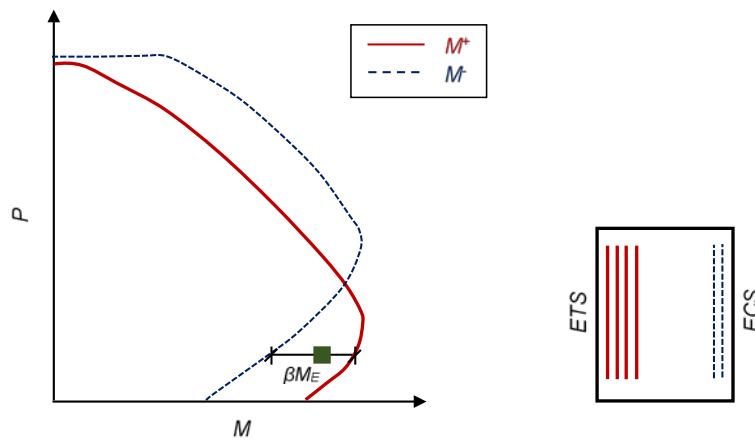


Fig. 3 – Representation of the factor β as $\beta.M_E = M^+ - M$ on the P - M Interaction Curve

The seismic performance of C-bent piers may be measured by residual displacements undergone by them in order to assess their reparability after damage in an earthquake. Residual displacements in a pier are governed by two major factors— (i) eccentricity of dead load from the centre of the pier and (ii) ductile capacity of the column. One of the methods proposed by past studies to reduce residual displacements is by increasing the amount of longitudinal tensile steel, thereby increasing value of the factor β . The current design proposals suggest a value of $\beta = 2$ for zero median residual displacements [2]. Due to dimensional constraints, if such a high value of β cannot be achieved, the maximum eccentricity for which the C-bent pier may be designed needs to be limited in order to reduce residual displacements. This paper aims at inspecting the seismic performance of C-bent piers with varying eccentricities in terms of residual displacements undergone in the event of an earthquake. This is achieved through seismic fragility analysis of C-bent piers by employing incremental dynamic analysis procedure. An attempt is made to identify the maximum eccentricity for which the C-bent piers may be safely designed.

2. Design and Modelling of Primary Components of the Bridge

2.1 Details of Bridge Structural Configurations

A typical configuration in which C-bent piers are used at places of turning of a bridge, as shown in Fig. 4, consists of a series of piers with increasing eccentricities connected to portal frames. The concrete girders resting on two bearings kept on each end on the pier cap have pinned connections on both ends in the transverse direction. In the longitudinal direction, they are assumed to have pinned connection on one end and rollers on the other to allow free expansion and contraction.



Fig. 4 – A typical configuration of eccentric C-bent pier with portal frame (Courtesy: www.tcpl.com [3])



In the present study, a system of three piers (P1, P2 and P3) and a portal frame (PF) was chosen to study the curved multi-span simply supported bridge to represent the turn of a metro viaduct. A 20 m wide four-lane road is considered with piers placed at the median of the road. The width of road, W , for one-way traffic is, therefore, 10 m. The superstructure is assumed to be a box-girder. A span length of 31 m is considered. The height of the pier is taken as 9 m. The depth of the column in the direction of eccentricity, D , is considered as 1.8 m, constrained by a 2.5 m wide median of the road. The depth of the column in the longitudinal direction of bridge is 2.4 m. These specifications of a C-bent pier are commonly used in Indian Metro viaducts [4].

The eccentricity ratios for C-bent piers and portal frames are considered as e/D and e/W , respectively, where e is measured from the median of the road to the centre of the two bearings on which the girder is placed. The whole study is conducted on seven e/D ratios for C-bent piers and four e/W ratios for frames adjusted in four configurations as mentioned in Table 1.

Table 1 – Eccentricity ratios of piers in different configurations of analytical model of the bridge

Pier No.	Eccentricity Ratios	C1	C2	C3	C4
P1	e/D	0.0	0.0	0.0	0.0
P2		0.0	0.0	0.125	0.25
P3		0.5	0.75	1.0	1.5
PF	e/W	0.2	0.5	0.6	0.8

2.2 Loading Conditions

For the design of C-bent piers, the dead load of the box-girder is taken as 3875 kN. The superimposed dead load is taken as 75 kN/m. The live load on the span including an impact factor of 1.2 is taken as 1224 kN. For the calculation of seismic load, earthquake response spectrum corresponding to zone IV and Type II medium soil is considered [5]. The importance factor and the response reduction factors for horizontal and vertical earthquake effects are taken as 1.5, 2.5 and 1.5, respectively [5,6]. Soil structure interactions have been ignored.

2.3 Design of Piers

The C-bent piers are designed to resist the axial forces, shear forces and bending moments arising in the structure due to dead load, live load and seismic load. The reinforcement of piers are designed individually in Section Designer of *SAP2000* (CSI 2018) [7] and checked using the 3-D P - M interaction surface as per IS 456 (BIS 2000) [8]. As mentioned earlier, the amount of reinforcement required is more on the *ETS* than on the *ECS* due to an increased tendency of deformation in the direction of eccentricity, which is dependent on the factor β . Yeow *et al.* (2013) [2] proposed a value of $\beta = 2$ to have zero median residual displacements of the C-bent piers.

It is notably difficult to achieve a high β and high e/D ratio on the P - M Interaction curve along with tension-governed failure, for a particular given cross-section of the C-bent pier. The only alternative is to increase the depth, D , of the pier which is restrained by the amount of space available for placement of piers on roads. Also, a value of $\beta = 2$ leads to requirement of large amounts of reinforcement for piers located in regions of low to medium seismicity which is uneconomical. Thus, a more realistic value of $\beta = 1$ is chosen for the design of C-bent piers.

All the piers are designed for the load combinations as mentioned before using value of $\beta = 1$. On the P - M Interaction curve, it is seen that with the increase in e/D ratio, the difference between the positive moment capacity, M^+ and the negative moment capacity M^- increases due to increase in M_E . Also, the balance



point moves closer to the design load P indicating that balanced failure is approached with increase in e/D ratio. For $e/D = 1.5$, the design loads and eccentric moments were quite large and the C-bent pier could not be designed within the tensile zone of failure. The reinforcement details of the piers with varying eccentricity are shown in Table 2.

Table 2 – Percent of tensile reinforcement (p_t) and compressive reinforcement (p_c) of designed C-bent piers

e/D	0.0	0.125	0.25	0.5	0.75	1.0	1.5
p_t (%)	0.41	0.47	0.58	0.71	0.89	1.25	2.18
p_c (%)	0.41	0.41	0.41	0.41	0.47	0.56	1.04

2.4 Finite Element Modelling

SAP2000 is used to develop numerical model of the primary elements of the bridge structure. M50 grade of concrete with unit weight of 25 kN/m^3 and Poisson's ratio of 0.2 is considered. 32 mm diameter bars of grade Fe 500 are used as reinforcement. Takeda's degrading stiffness model [9] and Mander's unconfined concrete model [10] have been used to establish stress-strain relationship. Spine model of the bridge has been developed where the pier, pier caps and girders are modelled as two-noded beam column elements. Foundation is assumed to be rigid. 5% damping has been considered in the study. Fig. 5 shows the model which has been used to study the seismic behavior of bridge configurations.

For non-linear analysis, P - $M2$ - $M3$ hinges have been considered at the base of the piers at location of maximum bending moments. The length of plastic hinge considered is $D/2$ as per ASCE 41 (2013) [11]. Fibre hinges obtained using section designer in *SAP2000* are used to model plastic hinge behavior. Non-linear dynamic analysis is conducted preceded by the dead load analysis using 'P-delta plus large displacements' option in *SAP2000*.

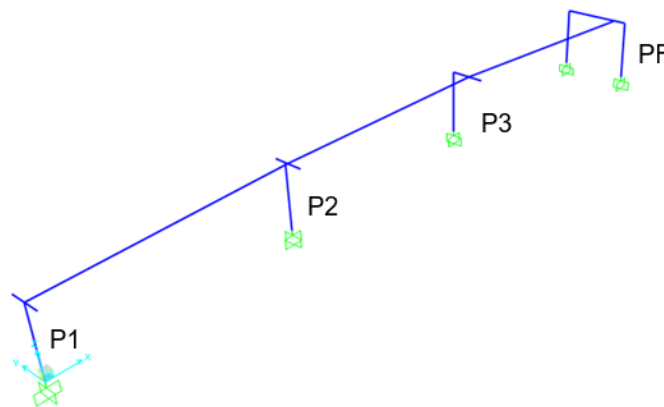
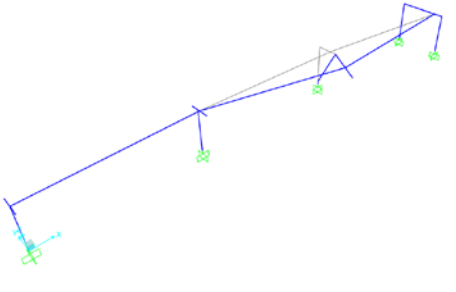
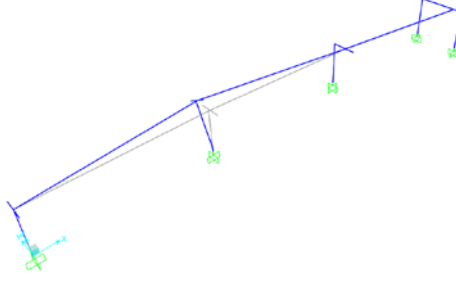
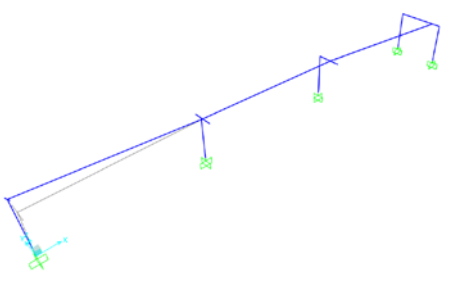
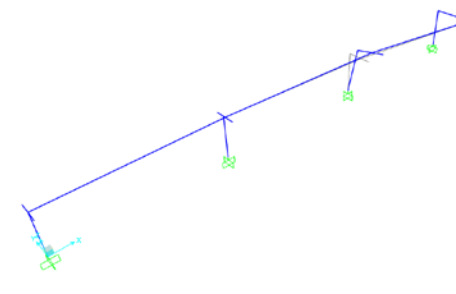
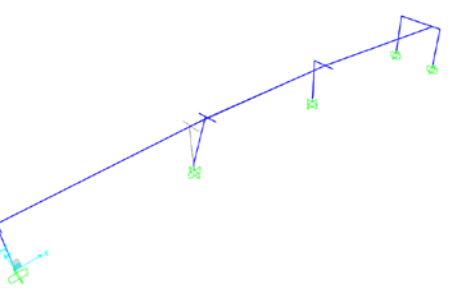
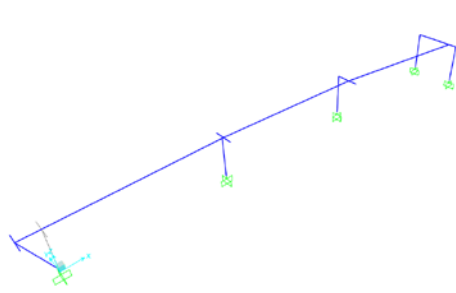
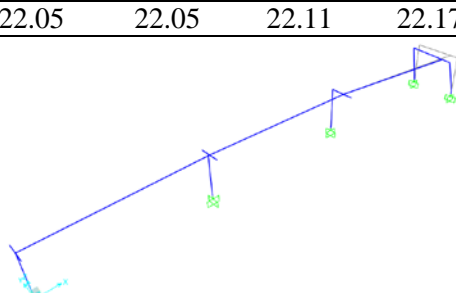
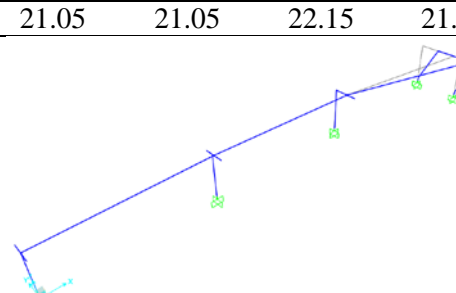


Fig. 5 – Finite Element Model of the bridge structure in *SAP2000*

2.5 Natural Period and Mode Shapes

In modal analysis, eight modes are considered for the present study such that the sum of modal mass participation ratios in both the longitudinal as well as the transverse directions is more than 90%. The natural period and modal mass participation ratio of the four bridge configurations are presented in Table 3, where T_i denotes natural period in i^{th} mode, 'T' indicates transverse mode and 'L' indicates longitudinal mode. The natural periods of the bridge configurations in various modes range between 0.187- 0.465 s. It is observed that transverse modes of vibration, which are in the direction of the eccentricity of dead load were more dominant. Also, the modes of vibration in the transverse direction are closely spaced. With increased eccentricity, more flexibility is introduced into the system. Therefore, the natural period of the system associated with C-bent piers increased with increase in its e/D ratios.

Table 3 – Natural period (T), modal mass participation ratio (Γ) and general mode shapes

Mode 1 (T) 					Mode 2 (T) 					
		C1	C2	C3		C4		C1	C2	C3
	T_1 (s)	0.425	0.429	0.443	0.465	T_2 (s)	0.422	0.422	0.429	0.430
	Γ (%)	21.51	20.95	20.13	18.5	Γ (%)	21.94	21.94	22.03	21.95
Mode 3 (T) 					Mode 4 (L) 					
		C1	C2	C3		C4		C1	C2	C3
	T_3 (s)	0.422	0.422	0.426	0.426	T_4 (s)	0.328	0.337	0.356	0.393
	Γ (%)	21.49	21.94	21.98	21.72	Γ (%)	22.03	22.01	21.92	22.27
Mode 5 (L) 					Mode 6 (L) 					
		C1	C2	C3		C4		C1	C2	C3
	T_5 (s)	0.320	0.320	0.326	0.328	T_6 (s)	0.256	0.320	0.323	0.323
	Γ (%)	22.05	22.05	22.11	22.17	Γ (%)	21.05	21.05	22.15	21.86
Mode 7 (L) 					Mode 8 (T) 					
		C1	C2	C3		C4		C1	C2	C3
	T_7 (s)	0.255	0.251	0.252	0.258	T_8 (s)	0.191	0.191	0.187	0.187
	Γ (%)	26.34	26.55	26.67	26.13	Γ (%)	26.62	26.64	26.77	26.47



3. Fragility Analysis

Seismic fragility of a structure indicates its susceptibility to get damaged under an earthquake ground motion of a given intensity. It indicates structural damage under a given seismic hazard given in terms of ground motion parameters such as peak ground acceleration or seismic intensity. A fragility curve, developed using Eq. (2), describes the probability of exceedance of a given damage state under a particular seismic hazard.

$$P_f = \Phi \left[\frac{S_d}{S_c} \geq 1 \right] \quad (2)$$

where P_f stands for the probability of surpassing a specified damage state, S_d is the mean structural demand and S_c is the mean structural capacity. The damage state denotes a particular performance parameter such as maximum displacement/drift/plastic rotation, residual displacement/drift, *etc.* In the current study, fragility analysis is conducted using incremental dynamic analysis (IDA) procedure.

3.1 Incremental Dynamic Analysis

IDA provides a tool for quantification of building seismic performance factor and has also been included in FEMA P695 (2009) [12]. It involves performing nonlinear dynamic analysis by subjecting a structural model to monotonically increasing intensity of applied ground motion in order to force it from elastic range to global collapse.

For performing IDA, a set of 20 ground motions obtained from Pacific Earthquake Engineering Research Centre (PEER) database is used. All the records have relatively high magnitudes ranging from 6.5-7.6, recorded on either stiff soil or soft rock sites. Overall, they represent far-field motions on firm soil site. Normalization of ground motion was done using FEMA P695 methodology by factoring them up or down to remove unwarranted variability in records sure to their magnitude, source type, distance from source and site conditions while maintaining their inherent record to record variability. The ground motions were further scaled by a global scale factor of 2.65 to match the acceleration response spectrum of IS 1893 (Part 1) [5], as shown in Fig. 6, and by a hazard factor of 0.1g-1g with 0.1g increment, representing PGA levels of ground motions. The 20 scaled ground motions were then applied to the four bridge configurations at 10 PGA levels each. Non-linear time history analysis was performed to obtain residual displacements undergone by piers of varying eccentricity in the transverse direction.

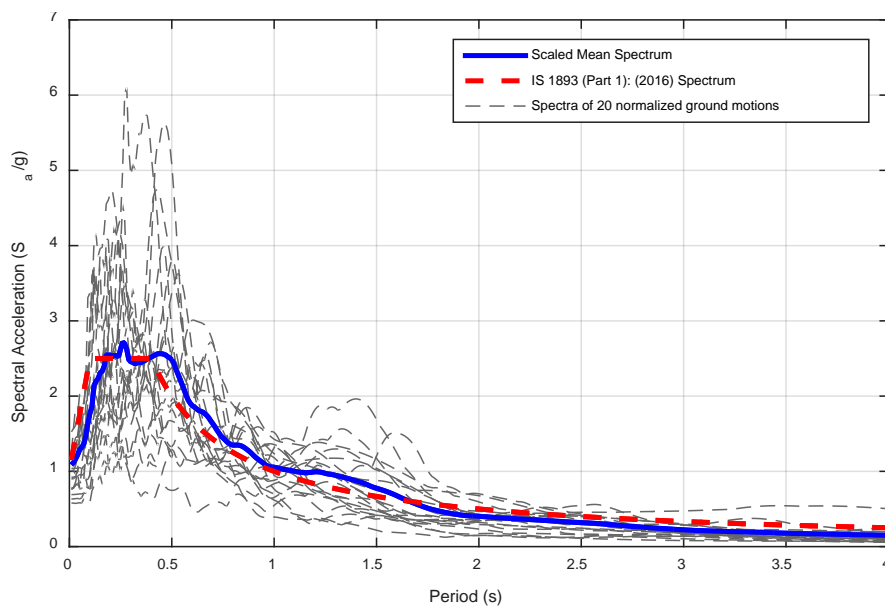


Fig. 6 – Comparison of acceleration response spectra for scaling of ground motions



3.2 Damage Characterization

Residual displacements undergone by the pier are critical to decide the retrofitting scheme to be employed to repair the structure. The damage state thus considered in the study is transverse residual displacement undergone by the C-bent pier after the application of earthquake ground motion.

To determine the capacity of the structure for fragility curve development, quantification of damage state is required. Bohnhoff [13] mentioned that the maximum deviation from the plumb for vertical members should not exceed 1%, which can be treated as a repairable limit for piers. ASCE 41 [11] also permits a value of 0.005 for plastic rotation for Life Safety level of structural performance for columns. FEMA 273 [14] allows 0.5% permanent drift for shear failure governed concrete walls and 1% permanent drift for vertical elements in concrete frames. Japanese Road Association (1996) [15] also recommends a limit of 1% on permanent drift in concrete bridge piers [16]. Therefore, two damage states have been considered in the study as given in Table 4.

Table 4 – Residual transverse drift capacity (damage state) of the C-bent piers

Damage State	Residual Transverse Drift
DS_1	1.0 %
DS_2	0.5 %

3.3 Regression Analysis

For a particular C-bent pier at a particular PGA level, seismic demand (S_d) for transverse residual drift obtained from IDA is divided by the seismic capacity (S_c) as defined by the quantified damage state. Regression analysis is then performed on $\ln(S_d/S_c)$ values and mean (λ) and standard deviation (σ) of $\ln(S_d/S_c)$ are expressed in terms of $\ln(\text{PGA})$. The cubic regression curves, as shown in Fig. 7 for one particular case, provided a good fit on the values of λ and σ . Probability of exceedance of a particular damage state indicating failure is obtained by the Eq. (3) assuming that natural logarithm of S_d/S_c (λ) follows normal distribution with standard deviation σ .

$$P_f = P\left(\frac{S_d}{S_c} \geq 1\right) = 1 - \Phi\left(\frac{\ln(1) - \lambda}{\sigma}\right) = \Phi\left(\frac{\lambda}{\sigma}\right) \quad (3)$$

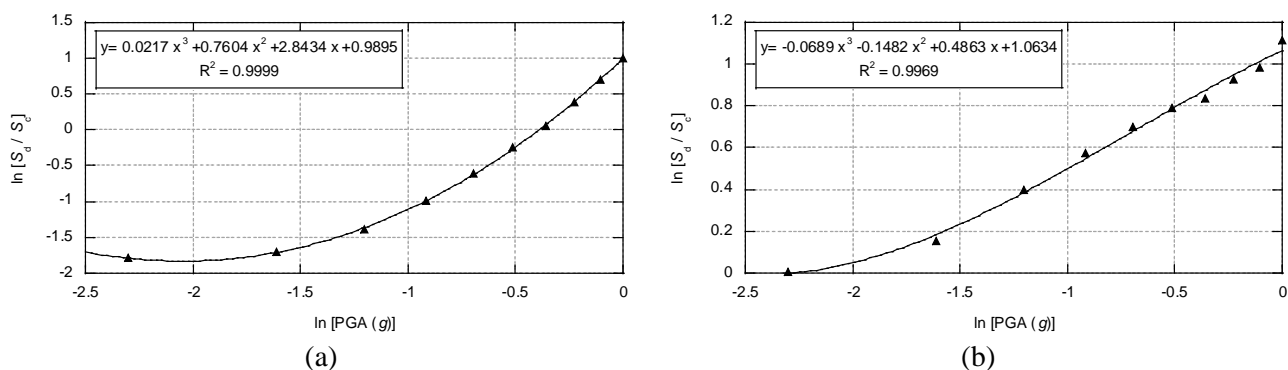


Fig. 7 – Regression curves of S_d/S_c with $\text{PGA}(g)$ on log-log scale for (a) λ and (b) σ for $DS_1 = 1.0\%$ for $e/D = 0.5$.

3.4 Fragility Curves

The probability of exceedance of a particular damage state obtained from Eq. (3) is used in the development of fragility curves for C-bent piers with varying eccentricity which are presented in Fig. 8. A collapse



probability of 50% is considered to analyze the seismic performance of structure. FEMA P695 suggests that probability of failure due to maximum considered earthquake (MCE) shall not exceed 10% and can be increased upto 20% to account potential “outliers” in acceptability criteria. Therefore, the C-bent piers are checked for three probability of exceedance of damage states— 10%, 20% and 50% and the collapse PGA corresponding to these collapse probabilities are presented in Fig 9.

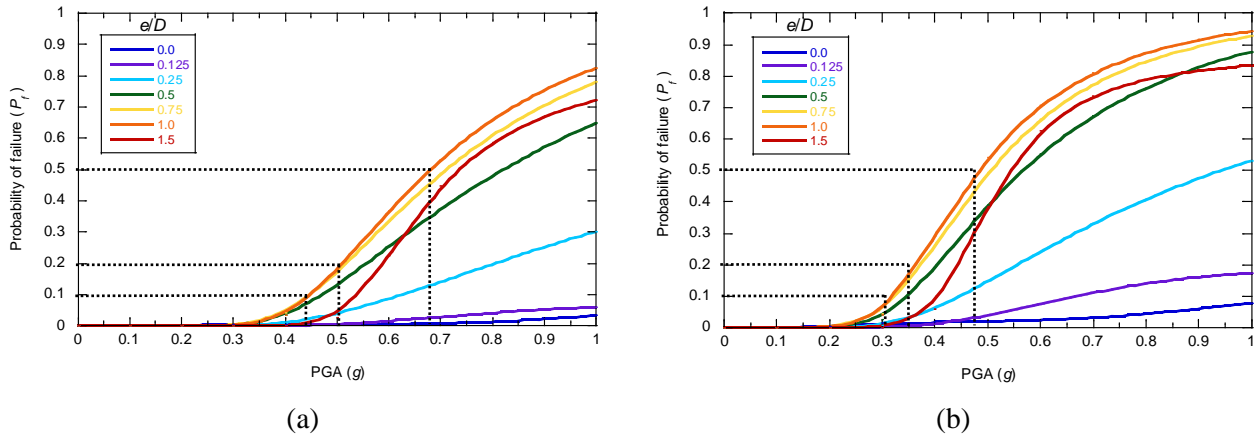


Fig. 8 – Fragility Curves of C-bent piers with varying eccentricity for (a) $DS_1 = 1.0\%$ and (b) $DS_2 = 0.5\%$

From Fig. 8, it is observed that the collapse probability for C-bent piers increases with increase in eccentricity ratio at a particular PGA level, except for $e/D = 1.5$. For low PGA levels, the difference in fragility is insignificant. All the piers perform well for very low levels of PGA corresponding to seismic zone II and III of India having design PGA of $0.10g$ and $0.16g$, respectively. However, the difference becomes substantially large when the PGA levels increase. For C-bent pier with $e/D = 1.5$, the collapse probability is even lower than that for $e/D = 0.5$. This is because the C-bent pier with $e/D = 1.5$ is extremely stiff and undergoes lesser residual displacements due to large amount of reinforcement. For high PGA levels, this pier undergoes brittle failure, with large standard deviations in residual displacements. Hence, its collapse probability is less than that of $e/D = 1.0$ and $e/D = 0.75$ at a particular PGA level.

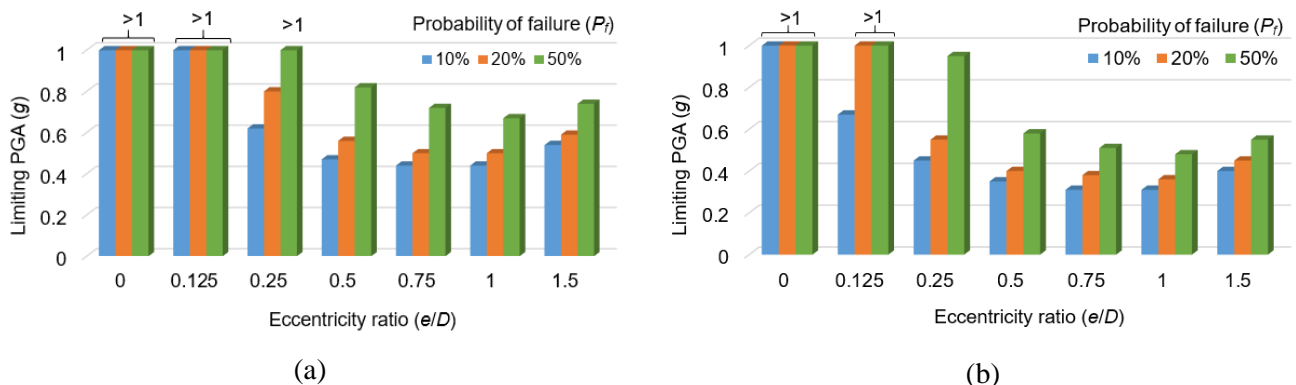


Fig. 9 – Limiting PGA levels for the three probability of failures as per FEMA P695 with increasing eccentricity ratios of C-bent piers for (a) $DS_1 = 1.0\%$ and (b) $DS_2 = 0.5\%$

There are two predominant trends that can be noticed in Fig. 9. The collapse probability increases with increase in PGA level for a particular e/D ratio. This implies that pier has higher susceptibility to fail at high PGA level. Also, the collapse PGA(g) decreases with increase in e/D ratio at a particular probability of failure. This means that a C-bent pier with higher eccentricity will fail at a lower PGA level for the same collapse probability. The most critical PGA level for safe performance of C-bent piers should be an envelope of all collapse PGAs, which is given by the collapse PGA of $e/D = 1.0$ as it is the lowest.



For the damage state $DS_1 = 1\%$ residual drift, the collapse PGA for $e/D = 1.0$ at 50%, 20% and 10% probability of failure are 0.67g, 0.50g and 0.44g. As the lowest collapse PGA (0.44g) for 1% drift limit is more than the highest design level PGA of 0.36g for seismic zone V in India, all the C-bent piers upto an eccentricity ratio of 1.0 perform well. This also reaffirms the adequacy of $\beta = 1$ for the design of C-bent piers. For the damage state $DS_2 = 0.5\%$ residual drift, the collapse PGA for $e/D = 1.0$ at 50%, 20% and 10% probability of failure are 0.48g, 0.36g and 0.31g. Thus, the C-bent piers designed for seismic zone IV of India with a PGA of 0.24g perform satisfactorily but the marginal safety is very low because the difference in collapse PGA is very low, that is, 0.07g. Since for a stricter damage state of 5% drift, the collapse PGA (0.31g) is lower than that for seismic zone V (0.36g), the safe eccentricity ratio limit upto which the C-bent piers can be designed should be 1.0 for an acceptable performance of C-bent piers. From the structural specifications such as spacing between bearings on the pier cap, it is suggested that at least one of the two bearings supporting the girder at one end should be placed vertically above the pier while designing the curved track of the metro viaduct.

4. Conclusions

A study is conducted to find the seismic fragility of C-bent piers with varying eccentricity ratio. A value of $\beta = 2$ as proposed by past studies for zero residual displacements in piers was found to be unfeasible for a typical cross-section used in Indian metro viaducts. Thus, a more practically applicable value of $\beta = 1$ was used for the design of piers which was found to be satisfactory for a repairable damage of 1% residual drift. The effect of increasing eccentricity on fragility of C-bent piers was not significant at low PGA levels, but very prominent at higher PGA levels. For a residual drift limit of 1%, all the C-bent piers performed satisfactorily. However, for a stricter drift limit of 0.5%, the collapse PGA for $e/D = 1.0$ reduced from 0.44g to 0.31g which is lower than the design PGA of 0.36g as per Indian Seismic Code. Therefore, for a collapse probability of 10% as per FEMA P695, for a typical cross section of C-bent piers used in Indian metro viaducts, it is suggested that the highest possible eccentricity ratio for which the C-bent pier can be safely designed should be limited to 1.0. From structural specifications of the bridge components, a girder supported on two bearings at each end should be placed such that at least one of the bearings should be directly above the vertical column of the C-bent pier and the other bearing may rest on the overhang. The largest safe loading eccentricity for which this configuration is satisfied in the current study is equal to the depth of the pier in the direction of eccentricity, corresponding to $e/D = 1.0$.

5. Acknowledgements

An introductory overview of current design practices in Indian metro viaducts from Tandon Consultants Pvt. Ltd., New Delhi is sincerely appreciated.

6. References

- [1] MacRae GA (1994): $P-\Delta$ effects on single-degree-of-freedom structures in earthquakes. *Earthquake Spectra*, **10** (3), 539-568.
- [2] Yeow TZ, MacRae GA, Sadashiva VK, Kawashima K (2013): Dynamic stability and design of C-bent columns. *Journal of Earthquake Engineering*, **17** (5), 750-768.
- [3] TCPL (2019): Elevated Metro Structures. Tandon Consultants Pvt. Ltd. Retrieved in April 2019 from <https://www.tcpl.com/mrts.html>
- [4] TCPL (2018): Personal Communication.
- [5] BIS (2016): *Indian Standard Criteria for Earthquake Resistant Design of Structures – Part 1: General Provisions and Buildings*. IS 1893, 6th Rev., Bureau of Indian Standards, New Delhi, India.
- [6] BIS (2014): *Indian Standard Criteria for Earthquake Resistant Design of Structures – Part 3: Bridges and Retaining Walls*. IS 1893, Bureau of Indian Standards, New Delhi, India.



- [7] CSI (2018): SAP2000 - Integrated Finite Element Analysis and Design of Structures, Analysis Reference Manual. Computers and Structures, Inc., California, USA.
- [8] Bureau of Indian Standards (BIS) (2000). *Plain and Reinforced Concrete - Code of Practice*. IS 456, 4th Rev., New Delhi, India.
- [9] Takeda T, Sozen MA, Nielsen NN (1970): Reinforced concrete response to simulated earthquakes. *Journal of the Structural Division*, **96** (12), 2557-2573.
- [10] Mander JB, Priestley MJ, Park R (1988): Theoretical stress-strain model for confined concrete. *Journal of structural engineering*, **114** (8), 1804-1826.
- [11] ASCE / SEI 41-13, (2013): *Seismic Evaluation and Retrofit of Existing Buildings*. Structural Engineering Institute (SEI), American Society of Civil Engineers (ASCE).
- [12] FEMA P-695 (2009): *Quantification of Building Seismic Performance Factors*. Prepared by Applied Technology Council (ATC) for the Federal Emergency Management Agency (FEMA), Washington, D.C.
- [13] Bohnhoff DR (1998): Construction tolerances standard for post-frame buildings. *ASAE Meeting Presentation*, Paper No. 984027, St Joseph, MI, USA.
- [14] FEMA 273 (1997): *NEHRP Guidelines for Seismic Rehabilitation of Buildings*. Federal Emergency Management Agency, Washington, D.C.
- [15] JRA (1996): *Design Specifications of Highway Bridges, Part V: Seismic Design*. Japan Road Association, Tokyo, Japan.
- [16] Kawashima K, MacRae GA, Hoshikuma JI, Nagaya K (1998): Residual displacement response spectrum. *Journal of Structural Engineering*, **124** (5), 523-530.